Design of large diameter single drilled shafts supporting the 650-span structure for the REM project in Montreal using axial and lateral static load tests

Diab, R., Senior Geotechnical Engineer, SNC Lavalin
D'Amours, L., Vice President Business Development, SNC Lavalin
Zirmi, D., Geotechnical Project Manager, SNC Lavalin
Habib, J., Geotechnical Project Manager, Englobe

Paper prepared for presentation
at the Materials, Pavements & Structures Session

of the 2019 TAC-ITS Canada
Joint Conference
Halifax, NS

ABSTRACT

In 2018, the Caisse de Dépôt et Placement du Québec (CDPQ) awarded a $6.3 Billion Design-Build contract to the Joint Venture (JV) team NouvLR (led by SNC-Lavalin) for the design and construction of the Réseau Express Metropolitain (REM) in Montreal which will be one of the largest automated transportation systems in the world. Out of the 67 km network, over 25 km will be constructed on 650-span elevated structure founded on large diameter single drilled shafts socketed into rock. In order to optimize the design, the JV team agreed on performing two full-scale, bidirectional (Osterberg Cell) static load tests in two of the rock formations encountered along the alignment and two fully-instrumented lateral load tests in critical areas along the alignment: one in the cohesive soil of the Champlain Sea clay and the other in cohesionless soil.

In addition to a brief description of the construction procedure of the load test, this paper presents design details on the back-calculated side resistance value, a discussion on the displacement incompatibility of skin friction and end bearing, and a procedure to estimate a site-specific design value for the load transmitted to the tip. A simple method to estimate the ultimate shaft resistance in locations where the rock is of different quality than the rock at the load test location is discussed. As for the lateral load test, this paper presents a comparison of the lateral load test results with the lateral shaft response as simulated by LPile software, using *p-y* curve of API sand and Reese models for cohesionless soil; and API soft clay for the cohesive soil. The *p-y* curve as obtained from the pressuremeter tests performed in both cohesive and cohesionless soils are also compared to the lateral load test. The calibration of the design models to the load tests led to reliable foundation performance with shorter shafts, helping to reduce costs and mitigate construction issues associated with unnecessarily long shafts.

1 INTRODUCTION

Réseau Électrique Métropolitain (REM) is being constructed by a Joint Venture comprised of SNC Lavalin, Dragados Canada, Group Aecon Quebec, Pomerleau, and EBC, partnering with Aecom and SNC Lavalin as the lead design firms. The project, referred to as REM, is a fully automated light rail transit (LRT) proposed by the Caisse de dépôt et placement du Québec (CDPQ) Infra, to serve the major metropolitan areas in Montreal, Canada. Once completed, the 67 km REM will be one of the largest automated transportation systems in the world and will represent the largest public transportation infrastructure for the metropolitan area since the Montreal metro, inaugurated in 1966.

As shown on Figure 1, the new facility will link downtown Montreal, South Shore, West Island (Sainte-Anne-De-Bellevue), North Shore (Deux-Montagnes), and the Montreal-Pierre Elliott Trudeau International Airport.

The project comprises four segments: South Shore (SS) segment, with a total length of 15 km, will extend from downtown (Central Station) to the DIX30 commercial district passing across to Nuns' Island and then will use a rail deck constructed on the new Champlain Bridge (still under construction) to cross the St. Lawrence River. Over 3.5 km will be supported by an elevated structure. The Deux Montagnes (DM) segment will be mostly at grade and will consist of a direct conversion of the existing Deux-Montagnes line. The Sainte-Anne-De-Bellevue (SADB) segment will begin near highway A-13 and end at SADB Township with 17 km of elevated structure supported by

two abutments and 340 piers. The airport segment will divert from SADB line to make a stop in Technoparc St-Laurent before terminating at Montréal–Pierre Elliott Trudeau International Airport. The airport segment will include approximately 1 km of elevated guideway consisting of 2 abutments and 21 piers.

The foundation system for the structures will be single drilled shafts, socketed into sound rock. Depending on the structural loads and site conditions, the drilled shafts will range from 2.0 m to 3.2 m in diameter with embedment of up to 9.0 m within the sound rock.

As per the client (CDPQ) requirements, the design standards to be used for the geotechnical design are the Canadian Highway Bridge Design Code (CSA-S6-14), the Canadian Foundation Engineering Manual (CFEM 2006), and AASHTO LRFD Bridge Design Specifications (8th Edition, 2017), in decreasing order of precedence.

2 SITE GEOLOGIC CONDITIONS

The general geology of the layout consists of a till deposit overlying the bedrock at varying depths (2 to 17 m). The overburden soil overlying the till is mostly granular fill although clay deposits from the Champlain Sea up to 9 m in thickness is encountered in some areas, particularly along the SS and SADB segments. The surface of the bedrock is altered and fractured for depths varying from 1 to 3 m. Three rock types are encountered along the REM alignment: Limestone and dolomite along DM and SADB, and shale along the entire SS segment.

3 OBJECTIVES AND METHODOLOGY

In order to optimize the drilled shaft design and allow the use of higher resistance values, the JV team (NouvLR) agreed on performing one full-scale bidirectional (Osterberg Cell) static load test in each of the rock formations encountered in the project, namely limestone, dolomite and shale. However, since an O-cell test had already been performed in shale for the new Champlain Bridge project (also designed and constructed by a Joint Venture led by SNC Lavalin), an authorization from the Champlain Bridge project Joint Venture (Signature on the Saint-Laurent, SSL) to obtain and use the results of the load test was awarded. As a result, NouvLR performed one load test in dolomite and the other in limestone. The purpose of the tests was to determine the design values of side and base resistance at the ultimate limit state on drilled shafts constructed using means and methods which are identical to those to be used on production foundations. The results and analysis of the two load tests are presented in this paper. The results of the O-cell performed in shale are not presented as an authorization from SSL has not been obtained at this point.

It is of interest to note that another objective of the axial load tests was the development of an equivalent top load-settlement curve for production piles, calibrated with the results of the load tests. Such a curve could be used basically for settlement estimate at the serviceability limit state. The construction of the load-settlement curve is the subject of a separate paper still under preparation.

In many cases, particularly when the lateral structural loads are large, the design of drilled shafts is controlled by the lateral resistance provided by lateral support from surrounding soils and, depending on the soil condition and overburden thickness, by the rock socket. In order to optimize the lateral resistance design, the JV team decided to perform two full-scale lateral load tests. The

purpose of the test was to validate and calibrate the *p-y* curves as well as the lateral soil and rock parameters. The results and analysis of the lateral load tests are also discussed in this paper.

The selection of the lateral load test sites was determined in conjunction with the structural engineers based on structural loading conditions, overburden thickness, soil type and profile. Moreover, the drilled shafts tested for axial load were to be used as reaction piles and therefore, the selection of the site was also contingent on the rock formation.

After intensive investigation and examination of several candidate sites, one site was selected along DM segment where the rock is limestone and the overburden is mostly cohesionless soil and the other site was along SADB segment where clayey soil from the Champlain Sea is encountered and the rock is dolomite.

LPile version 2018 was used to simulate the lateral load tests. Several soil models were used to investigate the best suited models for the soils on site. At the SADB load test where cohesive soil is encountered, the results of the load test were compared to LPile results, but very large difference was immediately noticed regardless of the soil model. In fact, the lateral load test showed a much lower capacity than expected which led the design team to believe that some soil disturbance had occurred during construction. As a result, a second soil investigation was performed (2 weeks after the load test was completed) in order to reassess the soil parameters. The results of the second investigation showed the soil parameters correspond largely to the remolded soil parameters as explained below.

4 SUBSURFACE AND LABORATORY INVESTIGATION

Intensive soil and rock investigation was performed at the load test locations, which includes SPT boring, pressuremeter (in soil) and dilatometer (in rock), Cone Penetration Test (CPT), and Nilcon vane shear test in clay. The pressuremeter and dilatometer models used for the testing were the Texam model and the Probex model, respectively. The laboratory program consisted basically of sieve, hydrometer and Atterberg limits analysis of soil, unconfined compressive tests and elastic modulus in rock.

At the DM load test location, the borings indicated that the upper 3 m of the overburden consisted of fill material containing predominantly silty sand with an average SPT ‘N’ value of 6 blows/0.3 m, underlain by about 3 m layer of silty sand (glacial till) with an average SPT ‘N’ value of 18 blows/0.3 m. The rock consisted of limestone extending to the bottom of borehole at a depth of 12.10 m. The upper 0.75 to 3.2 m of rock was of very poor to poor quality with an average RQD of 28 percent. The bottom rock was good to excellent quality with an average RQD of 83 percent.

A pressuremeter test was performed at a depth of 4.35 m in the glacial till. The pressuremeter modulus was 5.41 MPa. The creep and limit pressures were 431 and 754 kPa, respectively. The dilatometer test showed an average dilatometer modulus of 12.2 GPa in the bottom good to excellent rock.

At the SADB load test location, the initial investigation (pre-construction of the test pile) indicated that the upper 4.35 m of the overburden consisted of clay deposit overlying 5.27 m thick layer of sandy and silty gravel (glacial till) with SPT ‘N’ values varying from 15 to 66 blows/0.3 m. The vane shear test performed in the clayey soil showed an upper 1.4 m clay layer with undrained shear

strength S_u of about 70 kPa underlain by 3 m clay with an average S_u of 50 kPa. Measurements were taken at intervals of 0.5 m. The bedrock surface was comprised of poor quality, weathered metamorphosed conglomerate with some calcite veins in the upper 0.7 m with an RQD of 25 percent underlain by dolomite in poor to good quality which had an average RQD of 69 percent.

A pressuremeter test was performed in the clayey soil as well as in the glacial till. The clay, which was tested at 1.50 m, 3.00 m and 4.00 m, showed an average pressuremeter modulus of 4.27 MPa; and an average creep and limit pressures of 220 kPa and 390 kPa, respectively. In the glacial till, at a depth of 5.25 m, the pressuremeter modulus was 5.20 MPa; and the creep and limit pressures were 632 kPa and 1,740 kPa, respectively.

As explained below, the construction method used by the contractor caused remolding of the soil around the shaft tested for lateral load. This was noticed during the analysis when the results were compared to LPile model. As a result, additional soil investigation was carried out 2 weeks after shaft construction to verify the compactness of the overburden soils and the shear strength of the cohesive soils. The investigation consisted of SPT boring, CPT and vane shear test, all performed about 500 to 600 mm from the shaft.

The undrained shear strength (S_u) of the clay, as measured by the vane apparatus and confirmed by the CPT results, indicated an undrained shear strength of 24 and 9 kPa in the upper and lower clay layers respectively. The SPT N values in the glacial till were also slightly lower than the N value in the pre-construction phase. The results confirmed that the soils around the steel casing had been disturbed from their initial state.

A thorough examination of the rock quality through which the tested drilled shafts were constructed shows the following rock parameters:

	SADB	DM
- Rock type	Dolomite	Limestone
- Average RQD along the shaft:	69 percent	83 percent
- Average joint modification factor, α:	0.72	0.82
- Average intact rock modulus, E_i:	75.6 GPa	56.7 GPa
- Average dilatometer modulus, E_d:	12.2 GPa	12.7 GPa
- Poisson ratio, μ :	0.33	0.29
- Average unconfined compressive strength, q_u:	145 MPa	68 MPa
- Coefficient of discontinuity spacing, K_{sp}:	0.20	0.20
- Geologic Strength Index, *GSI*:	59	61

5 CONSTRUCTION PROCEDURE

A 1,300 mm diameter permanent steel casing was placed at the proposed shaft location. A hydraulic rig (LB 36-410) was used to insert the casing through the overburden and the fractured rock until refusal on the rock surface was reached. The overburden was excavated with an auger mounted on the drilling equipment. At the SADB site, before the installation of the casing the contractor carried out a pre-hole in the clayey soil with a 1,180 mm diameter auger in order to facilitate the casing placement.

A 1,180 mm diameter auger drilled the rock surface at the bottom of the steel casing with a minimum of 300 mm of recess. Once the shaft had been sealed, rock drilling was done with a rock-

drilling bucket. To obtain a relatively flat base on the rock surface, the sub-contractor used a cleaning bucket (KBF-K) to flatten the surface. The bottom of the rock socket of the shaft was cleaned with an airlift multiple times until the tolerance requirements were met. During the excavation and the cleaning of the soil inside the casing at SADB, the contractor decided not to adjust the water level in the casing with respect to the groundwater table. The casing was not filled with water to maintain a positive pressure head. At that time, no soil subsidence was observed on the surface. Figure 2 shows the placement of the casing and the reinforcement cage in the excavated hole.

After cleaning the base, the carrying frame with attached O-cell assembly (for the axially tested shaft) was inserted into the excavation and temporarily supported from the outer steel casing. The frame for the laterally tested shafts contained two inclinometer casings. Crosshole Sonic Logging (CSL) tubes were also attached to the interior of the reinforcement cage. A photograph of the frame with the O-cell assembly and the inclinometers are provided in Figures 3 and 4. The tremie pipe was then placed through the tremie hole. The rebar cage was inserted into the drilled shaft in a vertical position until the proper elevation was reached. Then the rebar cage was suspended to avoid the rebar cage siting directly at the bottom of the shaft.

Once the rock socket drilling was completed a sub-camera inspection device was used to confirm the rock socket base cleanliness using five spot sediment checking criteria (50 % less than 40 mm, no location exceeding 15 mm).

The concrete was pumped through a 5-inch O.D. diameter tremie line into the base of the shaft. During the concrete pouring, the volume of concrete in the pile was monitored as well as the volume that was poured from the delivery trucks combined with the concrete elevation which was measured on site directly into the shaft. The tremie pipe was held at least 3 meters in concrete at all times. Construction quality control involved concrete integrity testing using Ultrasonic Crosshole Testing (CSL) and pile integrity testing.

6 LOAD TEST RESULTS AND PROCEDURES

The general properties of the drilled shafts tested axially and laterally are as follows:

	SADB	DM
- Nominal pile diameter in soil and fractured rock:	1,300 mm	1,300 mm
- Nominal pile diameter in sound rock:	1,180 mm	1,180 mm
- Assumed concrete unit weight:	2,322 kg/m3	2,322 kg/m3
- Concrete compressive strength on the day of the test:	47.4 MPa	41.4 MPa
- Assumed concrete elastic modulus:	33,104 MPa	30,936 MPa

6.1 Axial Load Tests

The bi-directional static O-cell load tests on full-scale non-production test shafts were performed by LoadTest, Inc in accordance with ASTM D1143 Loading Procedure A – Quick Test. The tests were performed using one (1) 13.8 MN bidirectional embedded jacks (O-cell) to load the base area of the shaft against the side resistance of the socket above the base.

A summary of tested drilled shafts dimensions and elevations are as follows:

	SADB	DM
- Length of pile below bottom of O-cell plate:	100 mm	130 mm
- O-cell top plate diameter:	880 m	880 mm
- O-cell bottom plate diameter:	720 mm	720 mm
- Pile tip elevation	11.65 m	19.49 m
- Bottom of permanent casing elevation:	14.75 m	22.59 m
- Maximum bi-directional load applied to the pile:	20.53 MN	20.56 MN.

At the pre-award (proposal) phase, the preliminary analysis indicated that *L*/*r* ratio (where *L* is the socket length and *r* is the shaft radius) of 2 to 6 would be sufficient to support the ultimate (unfactored) structural loads for production piles (between 15 and 25 MN). For these ratios, the percentage of the total load transmitted to the shaft base was estimated to be in the range between 10 and 25 percent, based on CFEM (2006) as explained below. Therefore, both the load test method and the O-cell load capacity were selected such that the mobilized end bearing exceeds 10 to 25 percent of the total capacity. As a result, and in order to maximize the mobilized end bearing at lower cost, the concept known as the "Chicago Method", which consists of utilizing a smaller base area to maximize the unit base pressure, was used. This approach is particularly effective in testing shaft with limited rock socket embedment. Since the bottom O-cell plate is smaller than the upper one and much smaller than the shaft diameter, the base resistance acts against a 720 mm diameter area and the side shear reaction acts against a 1,180 mm diameter socket. A larger unit end bearing pressure is thus mobilized (See Section 7.1.2. below for details).

At the maximum load, the displacements above and below the O-cell were 3.56 mm and 9.58 mm, respectively in dolomite (SADB); and 2.04 and 14.18 mm, respectively in limestone (DM). Those displacements correspond to maximum downward and upward loads of 20.53 and 20.18 MN, respectively in dolomite (SADB); and 20.56 and 20.21 MN, respectively in limestone (DM). The upward load represents the net load which is defined as gross O-cell load minus the buoyant weight of the pile above. The load-displacement curves are shown in Figure 6.

Four levels of two sister bar vibrating wire strain gages were attached diametrically opposed to the reinforcing cage. The bottom two levels (Levels 1 and 2) were located in the rock socket area below the steel casing. Figure 7 shows the calculated unit skin friction versus pile vertical displacement in Zones 1 and 2 of the test pile, where Zone 1 is defined between the O-cell and strain gages in Level 1 and Zone 2 is located between strain gages Levels 1 and 2. The results show that the skin friction derived from the zones above the rock socket (along the steel casing) is negligible compared to the unit skin friction along the rock socket. Hence, the skin friction along the steel casing was neglected in subsequent analyses and recommendations, assuming that for the production pile steel casing penetrates through overburden soil and the fractured rock.

Since the bottom O-cell plate (just above the shaft base) is significantly smaller than the shaft base area, the scaling effect was considered to develop the displacement versus unit end bearing curves. For this perspective, the theory of elasticity was used to estimate the displacement of the entire pile base area (1.09 m^2) associated with the pressure applied at the bottom O-cell plate (0.41 m^2). In other words, the displacement that would occur at the pile tip was calculated as if the stresses at the bottom plate were applied over the entire base area.

Figure 8 presents the pile tip displacement versus the measured unit end bearing as well as the corrected end bearing estimated for the full base when the same pressure is applied. The mobilized skin friction curve is plotted on the same graph.

6.2 Lateral Load Tests

Lateral load tests were also performed on sacrificial drilled shafts by LoadTest, Inc. in accordance with ASTM D3966, Standard Test Methods for Deep Foundations Under Lateral Load. The drilled shafts tested previously for axial load (O-cell) were used as reaction piles and were located at about 6 m from the laterally tested shafts. In each tested shaft, two inclinometer casings were attached to the reinforcing cage and positioned at 90° to the direction of loading (See Figure 3). In each of the two casings, seven inclinometers (Geokon Model 6300 Series) were installed to monitor the variation of deflection and tilt response with depth. The depths at which the inclinometers were placed are indicated below. The hydraulic jack used to apply the load consisted of 330 mm diameter Osterberg Cell (O-cell) calibrated to 4996 kN. A W12x79 beam section connected the loading assembly to the reaction pile. Fifty millimeters thick steel plates were positioned between the loading apparatus and the pile to provide a flat, uniform loading surface (See Figure 5). The loading was applied in 10 increments and each successive load increment was held constant for a period of time in accordance with the ASTM Standard.

A summary of tested drilled shafts dimensions and elevations are as follows:

	SADB	DM
- Average ground surface elevation	26.85 m	32.49 m
- Pile tip elevation	13.75 m	19.49 m
- Bottom of permanent casing elevation:	15.15 m	22.59 m
- Level 0 to 7 inclinometers depths:	0, 1.7, 3.2, 4.8, 6.1, 9.3, 12.1	0, 1.5, 3.1, 4.6, 6.1, 7.7, 11.25

At the DM segment (cohesionless soil) the maximum lateral load applied to the pile was 2.0 MN with a maximum head deflection of 71.06 mm. The pile head rotation angle was 0.61° from vertical. At the SADB segment (cohesive soil) the maximum lateral load applied to the pile was 1.01 MN with a maximum head deflection of 66.60 mm. The pile head rotation angle was 0.54° from vertical. The load-displacement curves for both the tested and reaction piles are presented in Figure 9.

7 CALIBRATION OF AXIAL AND LATERAL RESISTANCE AGAINST TEST RESULTS

7.1 Axial Load Tests

Drilled shafts socketed in rock and subject to compressive loading are usually designed either in skin friction along the wall of the rock socket, end bearing on the material below the tip of the drilled shaft, or a combination of both. A decision by the REM design team was made to design the drilled shafts such that both the toe and side resistance are to be used for estimating socket capacity.

7.1.1 Skin Friction

A typical design approach for side resistance relates the unit side resistance, f_s and the square root of the unconfined compressive strength of the bedrock, $\sqrt{q_u}$. The method contained in Turner (2006)

originally dating back to Horvath and Kenney (1979), and normalized to dimensionless units is presented as Equation (1):

$$f_S = C.P_a.\sqrt{\frac{q_u}{P_a}} \quad (1)$$

Where P_o is the atmospheric pressure (101 kPa), C is an empirical constant and q_u is the unconfined compressive strength of the rock. In general, the lesser of the compressive strength of either the concrete or rock is used for the design.

The current edition of AAHTO 2017 recommends the use of a value of 1 for the parameter *C*, based on the most recent regression analysis of available load test data that is reported by Kulhawy et al. (2005) and that demonstrates that the mean value of the coefficient *C* is approximately equal to 1.0. A lower bound value of *C* = 0.63 was shown to encompass 90% of the load test results. The CFEM (2006), on the other hand, recommends a range of values between 0.63 and 1.41 reflecting the variability of test results obtained by different authors.

One of the objectives of the load test was to calibrate the empirical parameter *C* against the results of the O-cell test, at the project site for both limestone and dolomite.

The data on Figures 6 through 8 shows the maximum mobilized unit skin friction is 1.80 MPa for dolomite (SADB) and 1.87 MPa for limestone (DM). Based on these input values, the value of *C* in the equation above was back-calculated and found to be equal to 0.82 at SADB and 0.92 at DM.

It should be noted that the average unconfined compressive strength of the rock, q_u, at the site was 145 MPa and 68 MPa for dolomite and limestone, respectively. The strength of the rock substantially exceeded the 47.4 and 41.4 MPa compressive strength of the concrete used for the drilled shaft. As a result, the value of concrete compressive strength was substituted for q_u in the above equation.

It is also important to note that the measured side resistance was less than the nominal (ultimate) strength value due to the fact that concrete compressive strength on the day of testing was higher than the anticipated design concrete strength of 35 MPa. Therefore, any back-correlation using the measured values represents a lower bound value, since the test was limited by the capacity of the system. However, for the purpose of the analysis, the maximum measured mobilized unit skin friction was conservatively considered as the ultimate unit skin friction for the rock stratum. Thus, considering the ultimate resistance was not attained, the value of *C* is close to the value suggested by AASHTO.

7.1.2 Tip Resistance

The O-cell test results were also used to estimate the mobilized end bearing resistance. The ultimate end bearing is given in the CFEM (2006) by the following equation:

$$q_t = 3.K_{sp}.q_u.d \quad (2)$$

Where K_{sp} is the coefficient of discontinuity spacing which is a function of both spacing and aperture of rock discontinuities and *d* is a depth factor = 1+0.4 (L/D) ≤ 3.

The average q_u of the rock beneath the base of the test shaft was about 145 MPa for dolomite (at SADB) and 48.5 MPa for limestone (at DM). Using the equation above leads to nominal unit base resistance values of 175 and 60 MPa for dolomite (SADB) and limestone (DM), respectively, which largely exceed the mobilized end bearing of about 19 MPa. However, as mentioned above, the objective of the test was not to mobilize the full end bearing, which would require a larger O-cell capacity and completely different setup, but rather to mobilize 10 to 25 percent of the total load in order to simulate accurately the behavior of production piles.

The O-cell test results showed that approximately 8.8 MN for dolomite (SADB) and 4.9 MN for limestone (DM) were mobilized in end bearing at the vertical displacement at which maximum skin friction was mobilized (see Figure 8). Therefore, approximately 30 percent of the total resistance (29.3 MN) for dolomite (SADB) and 19 percent of the total resistance (25.1 MN) for limestone (DM) were provided by the end bearing at the displacement corresponding to maximum mobilized skin friction.

7.1.3 Design Implications for Skin Friction

In order to estimate ultimate unit skin friction in locations where the same rock formation is encountered but where the rock is of different (lower or higher) quality, the joint modification factor, α, which is a function of RQD and joint type (i.e., open vs. closed) was introduced into Equation (1) above as shown in Equation (3). Values of α were selected using the guidelines presented in Table 10.8.3.5.4b-1 in AASHTO (2017) based on O'Neill and Reese, 1999.

$$f_s = C_1 . \alpha . P_a . \sqrt{\frac{q_u}{P_a}} \qquad (3)$$

Where C_1 represents the ratio of C calculated above (0.82 at SADB and 0.92 at DM) to the value of α at the load test location (0.72 at SADB and 0.82 and DM (See Section 4 above), therefore the following values of C_1 are being used in the analysis:

C_1 = 1.14 for dolomite (SADB)
C_1 = 1.12 for limestone (DM)

In summary, the skin friction is scaled down or up proportional to the ratio of α of the rock at a specific site location to the value of α obtained for the rock at the load test location. In other terms, for areas where the rock has higher (or lower) quality with joint modification factor higher (or lower) than the rock quality at the load test location, the unit side friction is multiplied by the ratio α at the proposed site to α at load test location.

7.1.4 Design Implications for Tip Resistance

Since the end bearing resistance mobilizes at large displacements compared to skin friction, only a fraction of the ultimate end bearing is used in the overall axial resistance of the drilled shaft. Therefore the total ultimate axial resistance of a drilled shaft socketed into rock corresponds to mobilization of the full available side resistance plus a fraction of the available base resistance. The proportion of the load reaching the base must then be estimated. To estimate the tip contribution to the total ultimate axial capacity, the displacement incompatibility of skin friction and end bearing was considered, as mentioned above.

The CFEM (2006) recommends the use of the Pells and Turner (1979) approach that is based on the theory of elasticity, to determine the load distribution between the end bearing and side shear. As expected, the longer the embedment depth into sound rock (rock socket), the smaller the load reaching the socket base. Also, the smaller the ratio of concrete modulus to rock mass modulus E_c/E_r, the smaller the tip resistance contribution.

At the load test locations where the ratio of *L/r* was equal to 5.2 and E_c/E_r was equal to 2.7 in dolomite and 2.4 in limestone, the Pells and Turner approach shows that approximately 8 percent of the total resistance would be taken by the end bearing for both limestone and dolomite, whereas the O-cell test results showed that approximately 19 percent for limestone (DM) and 30 percent for dolomite (SADB) of the total resistance was provided by the end bearing at the displacement corresponding to maximum mobilized skin friction.

In order to calibrate the tip resistance contribution for different *L/r* ratios and different rock qualities, the load test results were used to lay out the best estimate curve for E_c/E_r=2.7 (dolomite) and 2.4 (limestone) on the Pells and Turner graph, as shown on Figure 10 (red curves). The curves were multiplied by a factor equal to 0.7 to introduce a safety margin. For the range of possible *L/r* ratios to be used for production shafts of 2, 4, and 6, the tip resistance contribution for limestone would be 33, 16, and 11 percent, based on the load test calibrated curve, whereas the tip contribution estimated from the Pells and Turner approach would be 27, 11 and 7 percent, respectively. As for dolomite, for the same *L/r* ratios the tip resistance contribution, based on the load test plotted curve, would be 44, 26, and 20 percent whereas the tip contribution estimated based on the Pells and Turner approach would be 25, 10 and 5 percent, respectively.

Therefore, for the purpose of optimizing the design and estimating the tip resistance contribution for production piles where the shaft diameters, socket lengths, rock qualities and *L/r* ratios could be different, the tip resistance obtained from Pells and Turner curves would be multiplied by an adjustment factor equal to:

Limestone	• 1.2 for *L/r* = 2	Dolomite	•1.75 for *L/r* =2
	• 1.4 for *L/r* = 4		• 2.60 for *L/r* =4
	• 1.6 for *L/r* = 6		• 4.0 for *L/r* = 6

It is of interest to mention that the magnitude of load transferred to the tip based on Kulhawy and Carter (1992) approach (adopted by the FHWA) compares relatively well with the load test results.

7.1.5 Design Resistance Factor

One of the purposes of the load tests was to use the highest reasonable resistance factor allowed by the Canadian Highway Bridge Design Code. Since only three load tests (including the load test performed for the Champlain Bridge project in shale) were to be used for a total of 650 shafts (about 0.5 percent), calibrating the load test results to different rock qualities, *L/r* ratios, and shaft diameters was necessary to provide the level of confidence needed to use high resistance factors. A resistance factor of 0.6 was used for production piles when the applicable boring was drilled within 3 to 4 m from the center of the shaft and when the rock quality (degree of brokenness) was more or less similar to the load test location. In cases where the rock quality was much different such as in

fault areas where the rock is completely fractured to a great depth, a resistance factor of 0.4 was used. An engineering judgment needed to be used to determine the appropriate resistance factor.

7.2 Lateral Load Tests

7.2.1 *p-y* criterion for Soil and Rock

The most common method of analysis used in the design of deep foundations for lateral loading is the *p-y* method, represented by the finite difference model implemented in the computer code COMP624 and more recently in LPile software. The analysis is based on replacing the soil around the pile by a set of nonlinear springs which provide the soil resistance *p* as a nonlinear function of the pile deflection *y.* The approach has been widely accepted because of its simplicity and ability to capture the essential aspects of pile behavior.

The lateral response of the soil was analyzed and calibrated against the lateral load test results. LPile version 2018 was used to compute the lateral deflection, moment and shear along the pile shaft using the following *p-y* soil models for the granular fill material and the glacial till:

- API Sand model: the *p-y* curve for this model is characterized by a hyperbolic curve with an ultimate resistance (P_u). The API Sand *p-y* spring is dependent on internal friction angle of the soil, φ, the soil unit weight, γ, the coefficient of lateral subgrade reaction, k_h and the pile diameter.
- Reese model for sand: the shape of the *p-y* curve for the Reese model consists of an initial linear stiffness followed by a parabolic curve up to a displacement of 1/60 of the pile diameter and then a linear portion up to the ultimate capacity. The parameters required to define the *p-y* curve are the same as the API model with slightly different k_h values.

The coefficient of lateral subgrade reaction k_h for the API sand and Reese models were determined as a function of the friction angle as recommended by the authors of the two methods and clarified in the LPile technical documentation.

The lateral response of the cohesive soil has been analyzed and calibrated against the lateral load test results using the following soil model:

- API Soft Clay model: The *p-y* curve for this model is characterized by a hyperbolic curve with an ultimate resistance (P_u). The API Soft Clay *p-y* spring is dependent on the undrained cohesion (S_{ur} for disturbed and S_{ui} for intact properties), the soil unit weight *(*, the strain factor, ϵ_{50}, the coefficient of lateral subgrade reaction, k_h, the J-factor and the pile diameter.

Also, for both the cohesive (SADB) and cohesionless (DM) soil, the *p-y* curve derived from the pressuremeter test results was also used for the calibration with the load test results: The pressuremeter data was converted to a *p-y* curve according to Baguelin et al (1978) method. The *p-y* curve as developed from the pressuremeter test is characterized by three linear segments with slopes of k_h, ½ k_h and zero. Where k_h is estimated based on the following equation, proposed by Baguelin et al. based on Menard theory for pile diameter larger than 0.6 m:

$$\frac{1}{k_h} = \frac{2.B_0}{9.E_m}\left[\frac{2.65.B}{B_0}\right]^{\alpha} + \frac{\alpha.B}{6.E_m}$$

Where E_m is the pressuremeter modulus and B_0 is a reference diameter equal to 0.6 m. The parameter α is an empirical coefficient that depends on the soil type and the ratio E_m/P_l (where P_l is the limit pressure) and varies from 0.25 for gravelly soil to 1.0 for over-consolidated clayey soil.

Both the fractured and sound rock was modeled using the Rock Mass model developed by Liang et al. (2009). According to the model the *p-y* curve is expressed by a hyperbolic curve defined in term of the spring modulus, K_i, and the ultimate resistance per unit length of shaft P_u. K_i and P_u are dependent on the rock unconfined uniaxial compressive strength, q_u, Geological Strength Index GSI, the Hoek-Brown material index, m_i, Poisson ratio, ν, the rock mass modulus, E_r, and the drilled shaft bending stiffness *EI*.

The bending stiffness of the tested shaft was calculated by the program using the as-built steel reinforcement of about 1 percent of the gross cross-sectional area for the tested drilled shaft, with a 19 mm thick steel casing. The calculated bending stiffness *EI* varied between approximately $2x10^5$ (cracked section) and $8x10^5$ kN-m^2 (full section).

7.2.2 Analysis of the results

The soil and rock parameters used in LPile software, at the load test performed in the cohesionless soil (at the DM segment) and cohesive soil (at SADB the segment) are summarized in Tables 1 through 4. The rock parameters are obtained from laboratory testing and rock structural description.

In order to simulate the load test with LPile, the lateral displacements obtained in four of the load test increments were imposed in LPile at the pile head. The resulting shear forces at the pile head were then compared to those obtained by the load test.

For the cohesionless soil at DM, the deflection profile as obtained by the LPile for the API sand and Reese models as well as the pressuremeter data were plotted against the deflection profile of the test pile generated from the inclinometer data as shown on Figure 11. The figure also shows the shear forces versus displacement at the pile head obtained by simulating the soil with the two models as well as by the *p-y* curve obtained from the pressuremeter data.

It can be seen that the deflections along the pile shaft as obtained with the three methods are similar and match well with the load test deflection curves. Moreover, the point of fixity, for this particular case, is located about 1 m below the top of the fractured rock which indicates that the rock quality has only minor effect on the lateral behavior of the shaft. It can also be concluded that, for deflections less than about 25 mm, the API sand and Reese models seem to slightly over estimate the lateral soil response whereas the pressuremeter test matches well with load test results. As for large displacements (larger than 25 mm), the API sand is more in agreement with the lateral load test results to represent the behavior of the granular soil (fill and till).

As for the cohesive soil at SADB, the predicted lateral movement at the top of the shaft using the API Soft clay model described above and utilizing the remolded soil parameters was compared to the measured lateral movement from the test shaft as shown on Figure 12. For comparison purposes, soil parameters from the pre-construction phase (undisturbed), including the *p-y* curve obtained from the pressuremeter data, were plotted on the same figure to illustrate the disturbance effect on the shaft behavior.

It can clearly be seen that the lateral deflection and forces using the disturbed soil parameters, as obtained after construction, match almost perfectly with the results of the lateral load test. Furthermore, the results show the pressuremeter data tends to predict a slightly larger displacement for a given load than the API Soft clay model in the pre-construction phase. The point of fixity for this case also is located close to the top of the rock indicating that the rock quality does not affect the lateral behavior of the shaft, regardless of the soil model used in the analysis.

7.2.3 Design Implications

Since the API Sand and Reese models seem to slightly over estimate the lateral soil response for small deflections (less than 25 mm) and since the allowable lateral deflection at the ultimate limit state was limited to 25 mm for production piles, it was recommended that the k_h values for the API Sand and Reese models be reduced by about 5 percent to better represent the soil behavior at a small displacement. If pressuremeter data is available, the back-calculated *p-y* curve can capture quite accurately the soil response for small displacement with no required adjustment.

The API Soft Clay model predicts very well the lateral behavior of the shaft as illustrated by the simulation using the post-construction soil parameters. No soil parameters adjustment is required. Due to the disturbance of the soil at the SADB site, it was difficult to draw a reliable conclusion with regard to the behavior as predicted by the pressuremeter test. However, it seems that both the pressuremeter and the API Soft clay predict similar load-deflection curve at small as well as large displacement with the pressuremeter predicting slightly larger displacement.

8 SUMMARY AND CONCLUSIONS

The side resistance of the axial load tests in limestone and dolomite exceeded the capacity of the loading system due to concrete compressive strength, on the day of testing, higher than the anticipated design concrete strength, and therefore nominal strength value was not mobilized during the test. A back analysis of the measured side resistance suggests values of the empirical parameter *C* in the range between 0.82 and 0.92. However, considering the ultimate resistance was not attained, the relationships provided in the current FHWA guidelines and AASHTO appear to be reasonable with respect to estimating side resistance of drilled shafts in hard rock. The tip resistance contribution is larger than the contribution predicted by the elastic solution proposed by Pells and Turner that is adopted in the CFEM.

Calibrating the load test results, with regard to skin friction and load distribution, to different conditions (rock quality, shaft diameter and socket length) allowed the design team to use high resistance factors permitted by the Canadian Highway Bridge Design Code. Certain guidelines were developed for the use of the appropriate resistance factor.

The results from the lateral load tests were used as a basis to back-calculate the soil parameters that will result in the same movement at the top of the shaft utilizing LPile program. The load deflection curve at the top of the shaft was used as the reference in the back analysis. For both test shafts, the movement was resisted mostly by the overburden and slightly by the rock socket. The overburden consisted of granular material (granular fill over glacial till) at DM and cohesive soil (soft clay over glacial till) at SADB. API Sand and the Reese criterion were used to model the granular material and the API Soft clay was used to simulate the cohesive soil behavior. Moreover, the *p-y* curve as obtained from pressuremeter data was also analyzed. The Mass Rock model proposed by Liang et al.

was used to model the rock layers. Slight adjustments to the lateral subgrade reactions were suggested to be used to match the shaft top deflection at each load increment.

The load test performed in the cohesive soil showed the behavior of drilled shaft was very sensitive to remolding of surrounding soils. Instructions were given to the contractors to avoid subsidence or any soils disturbance, immediately around the steel casing by not performing any pre-holes during shaft construction and maintaining positive water head by keeping the water level inside the casing a minimum of 0.5 to 1 m above the ground water table.

9 ACKNOWLEDGMENT

The authors would like to thank the Design-Build Joint Venture (JV) team NouvLR for accepting our proposal for lateral and axial load tests. We are also grateful to the Caisse de Dépôt et Placement du Québec (CDPQ) for authorizing the publication of the load test results.

10 REFERENCES

American Association of State Highway and Transportation Officials (2017), *AASHTO LRFD Bridge Design Specifications*.

American Petroleum Institute, 2010. *Recommended Practice for Planning, Designing and Constructing Fixed Offshore Platforms - Working Stress Design, API RP 2A-WSD*, 21st Edition, Errata and Supplement, 2010.

Baguelin, F., Jézéquel, J.F., Shields, D. H., "*The pressuremeter and foundation engineering*" Trans Tech Publications, 1978.

Brown, D.A., (2008). "Load Testing of Drilled Shaft Foundations in Limestone, Nashville, TN." Research Report for ADSC – Southeastern Chapter.

Brown, D.A., Turner, J.P, and Castelli, R.J., (2010). "Drilled Shafts: Construction Procedures and LRFD Design Methods". FHWA NHI-10-016, May 2010.

Canadian Foundation Engineering Manual, 4th edition, Canadian Geotechnical Society 2006.

Canadian Highway Bridge Design Code (CSA-S6-14).

Isenhower, W. M., Wang, S-T, Vasquez, L.G. (2018) Technical Manual for LPile 2018.

Kulhawy, F.H. and J.P. Carter, "Settlement and Bearing Capacity of Foundations on Rock Masses," In Engineering in Rock Masses, F.G. Bell, Ed., Butterworth–Heinemann, Oxford, England, 1992, pp. 231–245.

Liang, R, K. Yang and J. Nusairat. 2009. "P-y Criterion for Rock Mass," *Journal of Geotechnical and Geoenvironmental Engineering,* American Society of Civil Engineers, Vol. 135, No. 1, pp. 26–36.

U.S. Department of Transportation, FHWA-NHI-18-024, Drilled Shafts: Construction Procedures and Design Methods

Table 1. Summary of Soil Parameters for DM Segment

		Soil Parameters	
Soil Type		Fill	Glacial Till
Thickness (m)		3.0	3.1
Friction Angle, ϕ (^{o})		30	32
Unit Weight Y (kN/m^3)		19	21
Coefficient of Lateral Subgrade Reaction (MN/m^3)	API Sand	13.0	15.0
	Reese	10.5	16.4
	Pressuremeter	13.1	15.2

Table 2. Summary of Rock Parameters for DM Segment

	Rock Parameters (DM)	
	Fractured Rock	Sound Rock
Rock Type	Limestone	
Compressive strength, q_u (MPa)	48.5	48.5
Geologic Strength Index (GSI)	22	45
Hoek-Brown index, m_i,	8.4	8.4
Poisson Ratio,ν	0.29	0.29
Intact Rock Modulus, E_i (GPa)	56.7	56.7

Table 3. Summary of Soil Parameters for SADB Segment

Soil Type	Thickness	Pre-Construction		Post-Construction	
	(m)	S_{ui} (kPa)	ϵ_{50}	S_{ur} (kPa)	ϵ_{50}
Upper clay	1.4	70	0.0079	24	0.0144
Lower clay	3.0	50	0.0095	9	0.0259
Glacial Till	Thickness	Φ (^{o})	γ (kN/m^3)	Φ (^{o})	γ (kN/m^3)
	2.0	33	9	28	8
	3.0	38	12	38	12

Table 4. Summary of Rock Parameters for SADB Segment

	Rock Parameters (SADB)
Rock Type	Dolomite
Compressive strength, q_u (MPa)	160
Geologic Strength Index (GSI)	61
Hoek-Brown index, m_i,	9.2
Poisson Ratio,ν	0.33
Rock Mass Modulus, E_r (GPa)	12.2

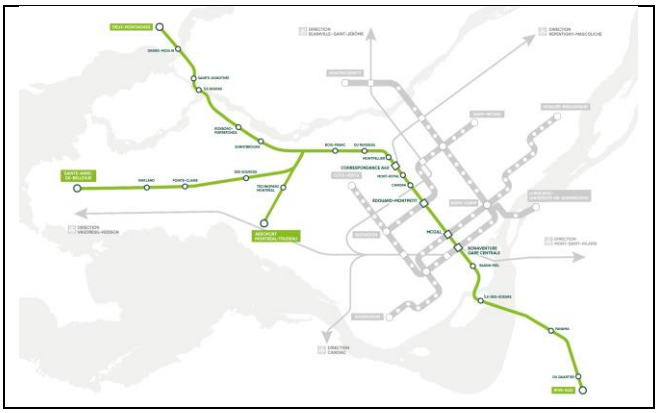

Figure 1: REM project alignment

Figure 2: casing and cage placement

Figure 3a: Rebar cage with inclinometers

Figure 3b: O-cell for lateral load test

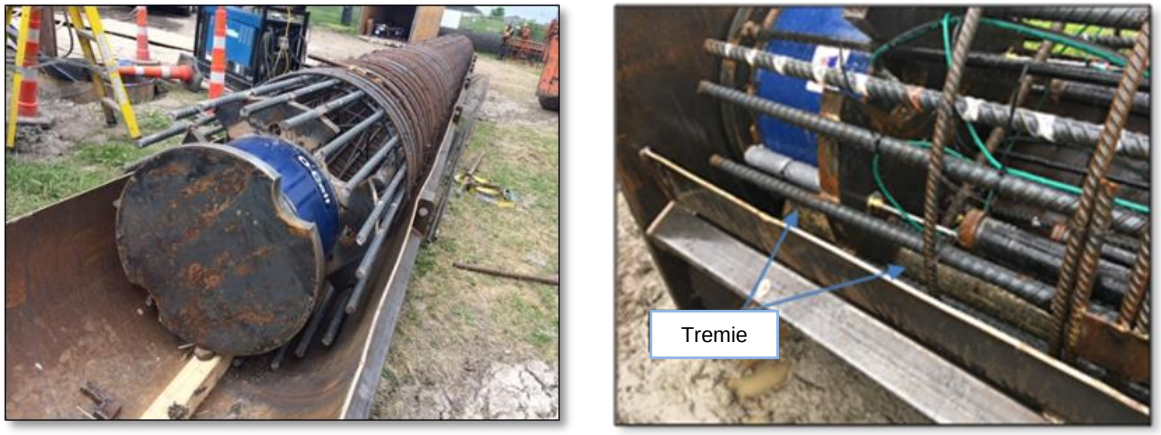

Figure 4: Rebar cage with attached O-cell

Figure 5: Lateral load test setup and assembly

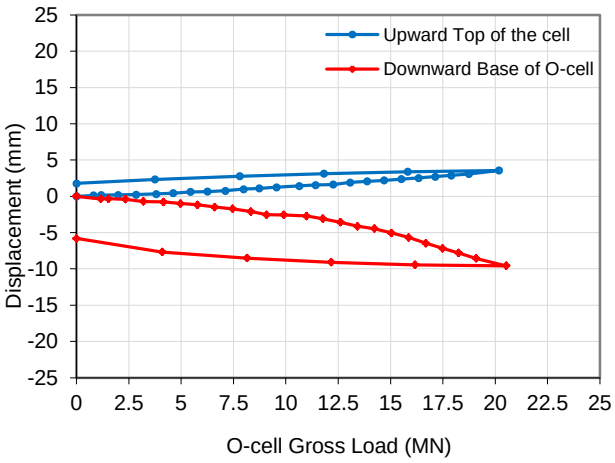

Figure 6a: O-cell Load-Displacement Curves in Dolomite (SADB)

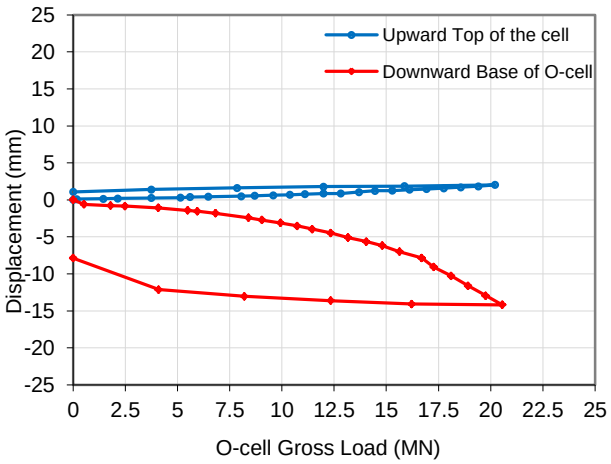

Figure 6b: O-cell Load-Displacement Curves in Limestone (DM)

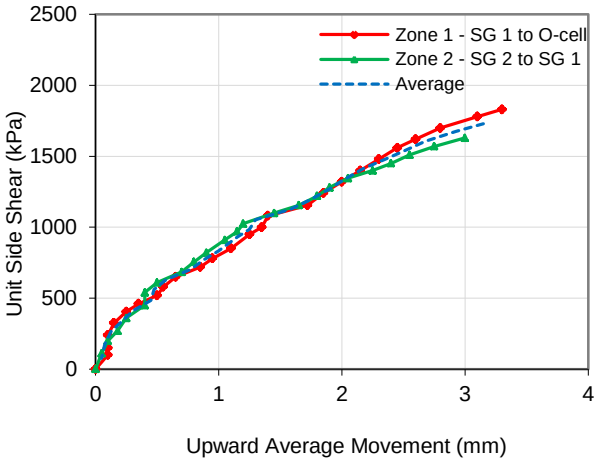

Figure 7a: Mobilized unit skin friction vs displacement in dolomite (at SADB)

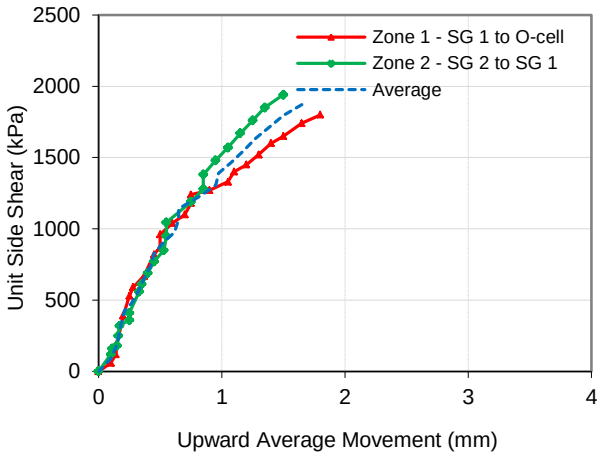

Figure 7b: Mobilized unit skin friction vs displacement in limestone (at DM)

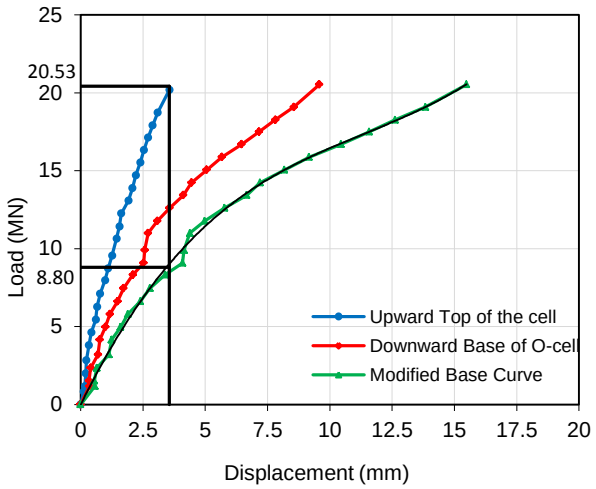

Figure 8a: Skin Friction and End Bearing from O-cell Test at SADB

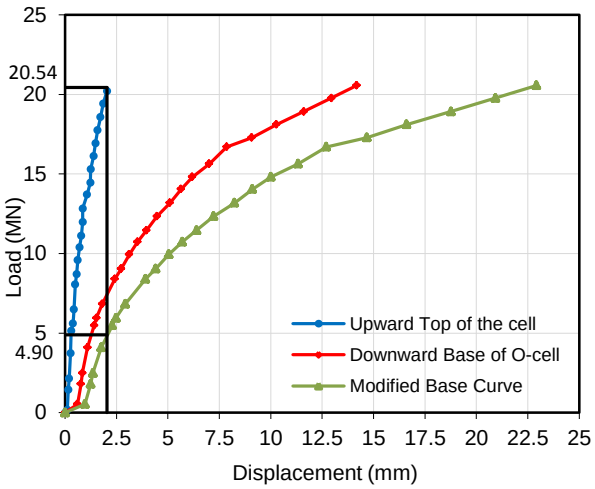

Figure 8b: Skin Friction and End Bearing from O-cell Test at DM

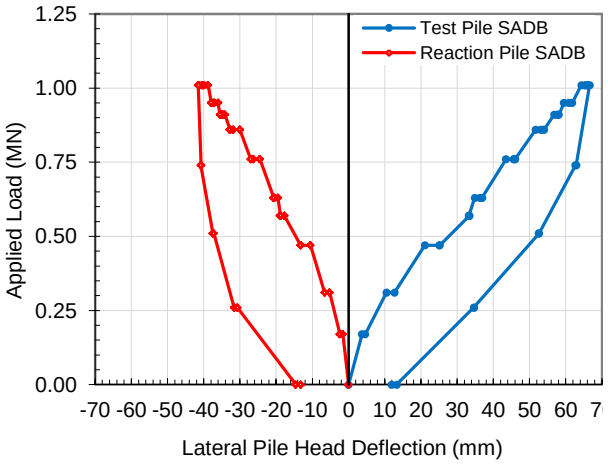

Figure 9a: Load-Displacement Curve for the cohesive soil (SADB)

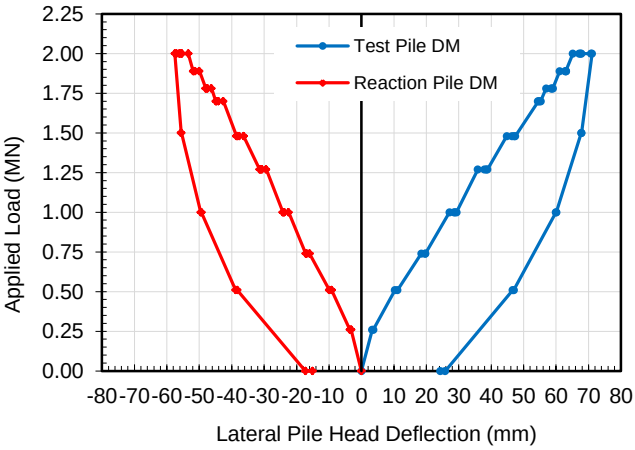

Figure 9b: Load-Displacement Curve for the Cohesonless soil (DM)

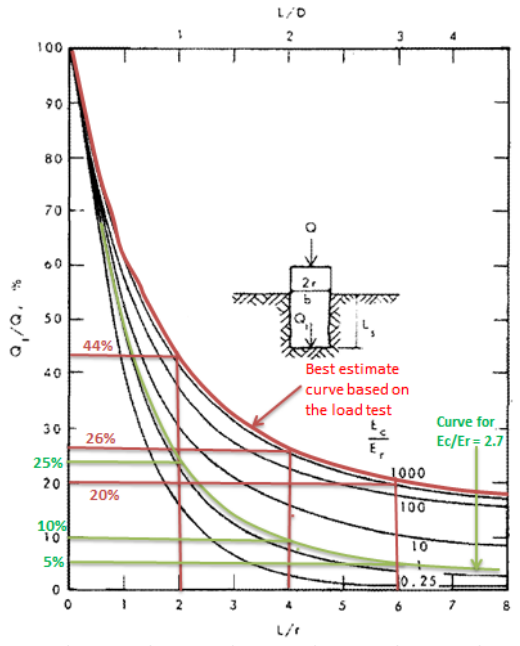

Figure 10a: Design Load Distribution in a Rock Socket for dolomite (SADB)

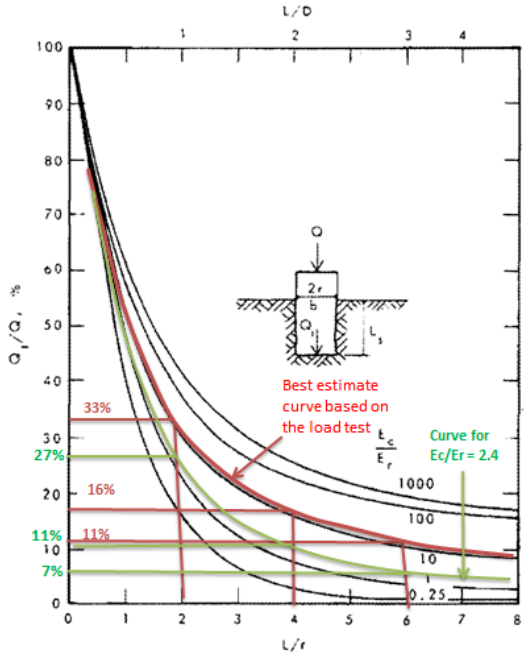

Figure 10b: Design Load Distribution in a Rock Socket for limestone (DM)

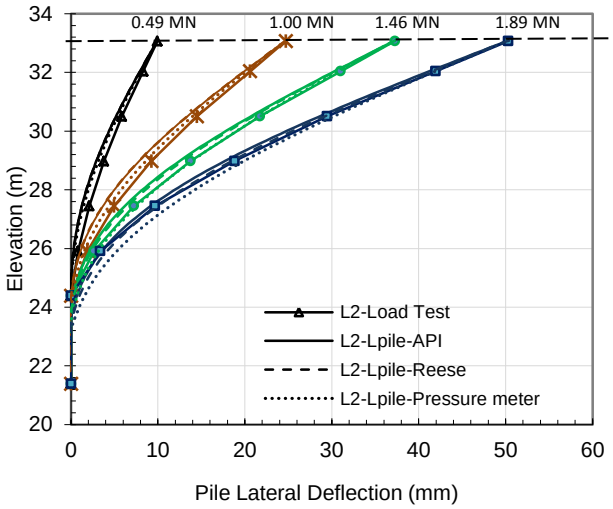

Figure 11a: Deflection profile at DM

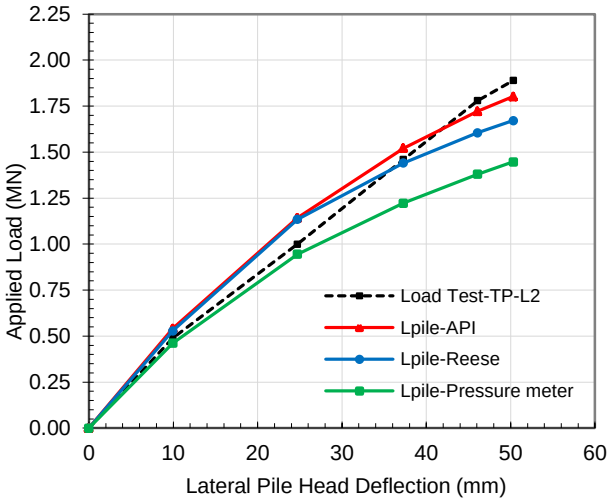

Figure 11b: Shear force vs deflection curves

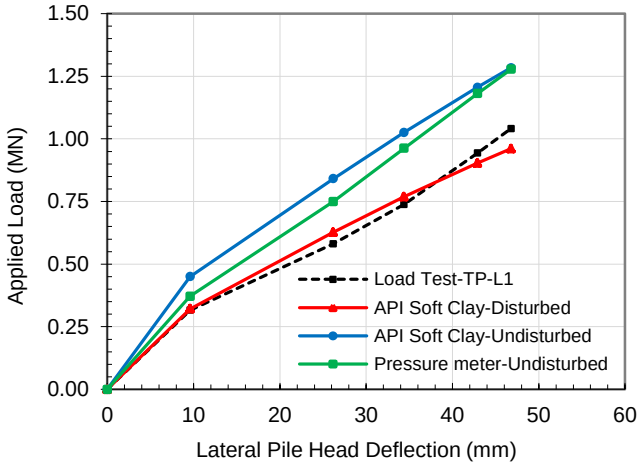

Figure 12: Shear forces vs deflection curves for the cohesive soil for remolded and undisturbed soil parameters at SADB